

Embedded ArUco: a novel approach for high precision UAV landing

Artur Khazetdinov

*Laboratory of Intelligent Robotic Systems (LIRS)
Intelligent Robotics Department
Institute of Information Technology and
Intelligent Systems
Kazan, Russia
ark@it.kfu.ru*

Aufar Zakiev

*Laboratory of Intelligent Robotic Systems (LIRS)
Intelligent Robotics Department
Institute of Information Technology and
Intelligent Systems
Kazan, Russia
zaufar@it.kfu.ru*

Tatyana Tsoy

*Laboratory of Intelligent Robotic Systems (LIRS)
Intelligent Robotics Department
Institute of Information Technology and
Intelligent Systems
Kazan, Russia
tt@it.kfu.ru*

Mikhail Svinin

*Information Science and Engineering Department
College of Information Science and Engineering
Ritsumeikan University
Kyoto, Japan
svinin@fc.ritsumeik.ac.jp*

Evgeni Magid

*Laboratory of Intelligent Robotic Systems (LIRS)
Intelligent Robotics Department
Institute of Information Technology and
Intelligent Systems
Kazan, Russia
magid@it.kfu.ru*

Abstract—This paper presents a novel approach for precise UAV landing using visual sensory data. A new type of fiducial marker called *embedded ArUco* (e-ArUco) was developed specially for a task of a robust marker detection for a wide range of distances. E-ArUco markers are based on original ArUco markers approach and require only ArUco detection algorithms. The applicability of developed markers was validated using UAV landing experiments in a virtual environment. Both a developed marker and a landing algorithm were implemented within the ROS framework and tested in the Gazebo simulator. According to our virtual experiments, an average landing accuracy was 2.03 cm with a standard deviation of 1.53 cm.

Index Terms—Fiducial marker, ArUco, ROS, Gazebo, UAV, PX4

I. INTRODUCTION

Modern unmanned aerial vehicles (UAVs) are actively used in different fields for military and civilian purposes. Typical tasks include searching for various objects in large areas [1], environment monitoring and control [2], structure inspection and monitoring [3], goods delivery [4], and others [5]. All these tasks require a UAV to take off at an operation start and to land after its task is completed. However, a precise landing without using global positioning systems (e.g., indoors) often requires a significant human intervention to ensure a successful landing. This becomes particularly important for critical

missions and in situations when a UAV carries an expensive equipment onboard since most of UAV crashes occur during a landing procedure and are caused by an unexpectedly hard landing [6]. Therefore, landing assistance systems are a common way to reduce a number of incidents. The problem of the precise landing could be resolved by improving an accuracy of a UAV's pose estimation.

A robot pose estimation based on visual sensory data is a key feature in many robotic applications: localization [7], robot navigation [8], SLAM [9] and others [10]. This process is based on finding correspondences between feature points in a real environment and their projection on a 2-dimensional image (e.g., from an optical camera). This process is computationally expensive for an arbitrary image. Therefore, synthetic fiducial markers are usually used for extraction of appropriate feature points [11]. A fiducial marker's predefined size and proportions allow to extract a relative camera rotation and estimate a distance to the camera. One of the most popular approaches is to use binary square-shaped fiducial markers [12] (examples of ArUco markers are shown in Fig. 1). An internal binary coding increases a detection reliability using automatic error detection and correction techniques. In this research, we used ArUco markers [13], which are very popular in augmented reality projects for assessing a camera



Fig. 1: Original ArUco marker with IDs 0, 1, 2, 3 (from left to right)

position [14]. The ArUco marker is a synthetic square-shaped marker, consisting of a wide black boundary and an internal binary matrix that encodes its unique identifier (ID). The black boundary speeds up a marker detection within an environment and encoded ID of the marker allows distinguishing different markers within a family of the markers. The internal binary matrix consists of $N \times N$ cells (entries) and each cell has a white or a black color.

A fiducial marker is placed on a landing surface. Next, during a landing process, a UAV needs to continuously detect the marker and move accordingly. Thus, the marker must be detected throughout the entire landing process, which means it should stay all the time within a camera angle of view. This requirement is hard to meet using standard fiducial markers: on the one hand, a large marker is easier to detect from a long distance; on the other hand, at a short distance a large marker area exceeds the camera field of view (and even partially leaves it) when the UAV approaches it close enough, which means the marker is not entirely captured by a video stream frames of the camera any more [15].

This article presents a novel approach that targets to resolve the problem of an accurate UAV landing using fiducial markers. It uses a modified ArUco marker, which we called **Embedded ArUco (e-ArUco)** marker. E-ArUco markers could be detected throughout an entire landing process, both from long and short distances, and the detection requires only the original ArUco detection algorithms. The proposed e-ArUco markers were tested using virtual UAV landing experiments with a PX4-based drone in the Gazebo simulator.

The rest of the paper is organized as follows. Section 2 presents a related work on a precise UAV landing. Section 3 describes the proposed system. Section 4 is devoted to the e-ArUco marker and the UAV precise landing algorithm. Section 5 demonstrates virtual experiments. We conclude in the last section.

II. RELATED WORK

Different UAV landing solutions were presented in research literature within the past decades. In [16], the author used AR Drone 2.0 UAV with two cameras for an indoor navigation and landing. ArUco markers served as reference points to perform an accurate localization. In cases when the markers were not visible, inertial measurements along with the Kalman filter were used to control the drone in order to achieve a required navigation reliability.

Authors of [17] presented two algorithms. The first algorithm concentrated on an ArUco marker detection within a UAV camera image, which allows to determine a position and an alignment of the UAV camera relatively to the marker. The second algorithm performed the UAV landing directly on the marker surface; it included a software module for adjusting a position of the UAV relatively to the marker in order to improve the landing accuracy. The developed algorithms were tested in the Gazebo simulator environment [18].

In [19] the authors also used an ArUco marker for a high precision UAV landing. In the proposed static and dynamic approach solutions, the UAV was equipped with an inexpensive Raspberry Pi camera and was capable of detecting ArUco markers of 56×56 cm size from a height of 20 m (static) to 30 m (dynamic). The method was validated using the ArduSim simulation platform [20] and experiments with a real UAV. The authors reported on an average offset of 11 cm from the target position and compared it with several other methods, emphasizing a rather low accuracy of a traditional GPS-based landing with their 1 to 3 m offset.

While most of the aforementioned authors have confirmed their approaches in artificial and real environments, their approaches did not detect ArUco markers throughout the entire drone landing process, which could improve landing accuracy.

Another way to improve a landing precision is to increase an accuracy and a reliability of onboard sensory systems [21]. However, this approach requires an additional hardware, increases a UAV cost, reduces versatility and genericity of the solution. Yet, since most of UAVs have onboard optical cameras, visual navigation could be integrated into their control loop with no hardware changes.

Wynn and McLain in [22] used a pair of nested ArUco markers to perform both a daytime and a nighttime landing of a UAV. An outer marker had a 70×70 cm size and contained 8×8 binary cells: an internal 6×6 matrix (that forms an ID) and an external black color boundary of a 1-cell width. The outer marker was placed on a white background and could be detected from a distance of about 17 m. In the center of the outer marker the authors placed a smaller inner marker of 12×12 cm size (8×8 cells marker consisting of the 6×6 cells internal matrix and a 1-cell width black color boundary), which could be detected from a distance of about 5 m and allowed to guide the landing process when the larger outer marker goes out of the camera's field of view. It should be noted, that at the distance of 1 to 2.5 m both markers were simultaneously successfully detected. The authors validated their approach with a set of experiments with 3DRobotics X8 multirotor with four sets of coaxial motors, Pixhawk 2.1 pilot system [23], and PX4 firmware [24]. FLIR Chameleon3 global shutter sensor camera with 1288×964 resolution, 78 degrees field of view and 3.6 mm M12 lens was set in a downward-facing manner and was responsible for marker detection and visual landing guidance. A real-time image processing and control were performed by an onboard NVIDIA Jetson TX2 with MAVROS being used to bridge Jetson and the Pixhawk. This approach is similar to ours, but it

had a number of drawbacks, which we succeeded to eliminate. The main drawback of the solution in [22] is the lack of correlation between outer and inner markers, which prevents a smart embedding that could be further multi-scaled. Moreover, since the inner marker overlaps four cells of the outer marker, this decreases a number of possible ID selections of both outer and inner markers as the foreground (inner marker) should be clearly distinguishable from the four cells of the background (outer marker).

III. SYSTEM SETUP

The PX4-LIRS UAV is a multirotor with four sets of motors, which was designed and constructed for research purposes of the Laboratory of Intelligent Robotic Systems¹ (LIRS) and uses Robot Operating System (ROS) [25] as a backbone of its software and control. The UAV is controlled using Pixhawk [23] with PX4 [24] firmware and Raspberry Pi 3. Raspberry Pi 3 was employed as the main computing unit of PX4-LIRS UAV and had several functions: it sends control commands to the UAV's flight controller using the MAVROS package [26], receives data from the optical camera and processes captured frames. ROS package *aruco_detect* detects ArUco markers in the camera images. The detection results are further used by the flight controller to determine a UAV movement direction. It uses Ubuntu Mate 18.04 and ROS Melodic [27].

ROS-based 3D dynamic Gazebo simulator [28] was used to validate the proposed approach of e-ArUco and the developed software in the virtual environment. We created a UAV model of PX4-LIRS UAV for the Gazebo simulator (Fig. 2), with the Pixhawk flight controller and PX4 software. A downward facing monocular camera was installed on the UAV model in order to detect ArUco markers on the landing surface under the UAV. The UAV's software was also imitated to simplify future software transfer from the Gazebo onto the real UAV. The built-in editor of the Gazebo allows creating 3D scenes without programming and includes a large library of ready-to-go 3D-models (an example is shown in Fig. 3). In addition to standard tools, there exist a number of cutting-edge tools and packages that were proposed by users and allow quick and easy Gazebo world creation [29].

IV. SOLUTION ARCHITECTURE

A. Embedded ArUco design

A novel e-ArUco marker (Fig. 4) is an ArUco marker that has an additional inner marker in the center of the original (outer) ArUco marker. The two markers (the outer and the inner) have different IDs. The main feature of the proposed solution is an ability to robustly detect the marker throughout an entire drone landing process. The outer marker is used for a rough drone positioning and the inner marker is used at late stages of the landing when the outer marker is too close to a camera and thus is not entirely captured by the camera frames of a video stream (since the marker area becomes too large

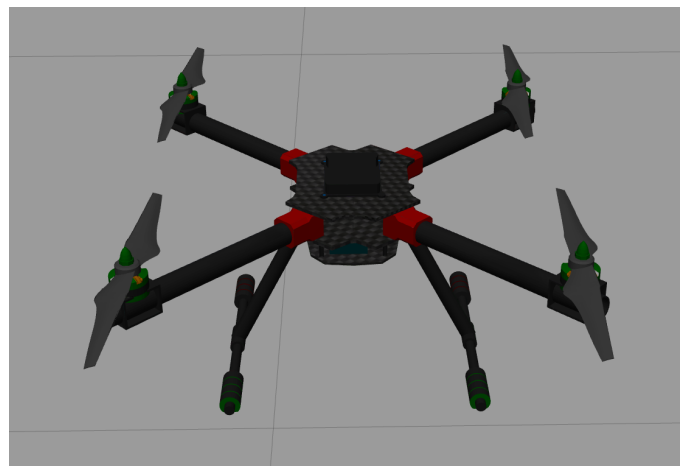


Fig. 2: The real PX4-LIRS UAV (top) and its model in the Gazebo simulator (bottom).



Fig. 3: A typical virtual environment created in the Gazebo simulator. The 3DR IRIS+ [30] and Hector [31] quadrotor models are located in the center of the stage.

¹<https://kpfu.ru/eng/itis/research/laboratory-of-intelligent-robotic-systems>

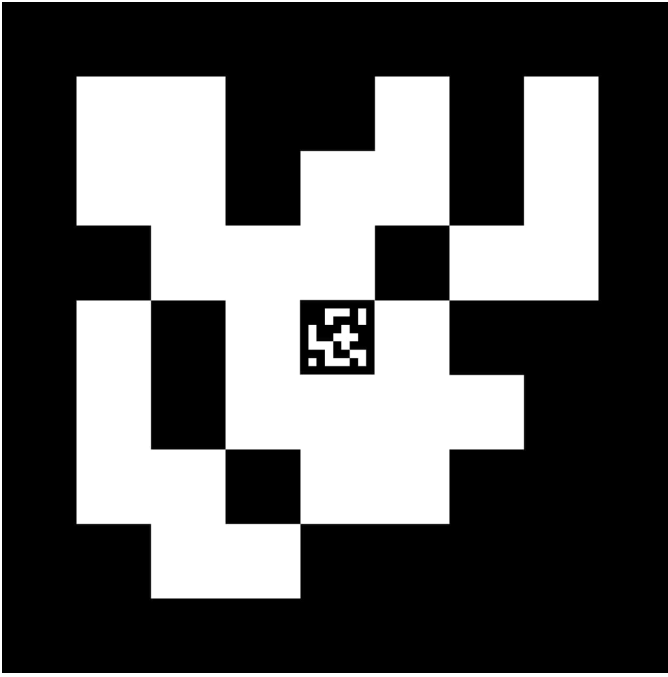


Fig. 4: Example of e-ArUco marker based on a 7x7-sized ArUco marker. The inner marker is located in the center of the outer marker, replacing the single black encoding square. The inner marker itself is a 7x7-sized ArUco marker.

and some of its area turns out to be outside of the frame). This feature improves the accuracy of landing as the e-ArUco marker becomes detectable all the way through the landing. When selecting a particular ID [32] for the outer ArUco marker, an attention should be paid that the inner ArUco marker replaces a single black "pixel" (a building block) in its center. Therefore the outer Aruco marker ID selection is limited to the ones with a black block in the center, while it is recommended to select an inner Aruco marker in a such way, that a number of its black pixels dominate over the number of white ones. The experimental setup used in this paper consisted of two ArUco markers of 45x45 cm size for the outer marker and 5x5 cm size for the inner marker. Table I describes minimal and maximal distances that allow a marker detection for inner ArUco, outer ArUco, and e-ArUco markers. The e-ArUco marker has the best performance as it could be detected from a distance of 0.2 m to 30 m.

TABLE I: Minimum and maximum detection ranges for original ArUco and e-ArUco markers.

Name	Size, cm x cm	Detection range, m	
		Minimum	Maximum
Inner ArUco	5 x 5	0.2	1.3
Outer ArUco	45 x 45	0.8	30
e-ArUco	45 x 45	0.2	30

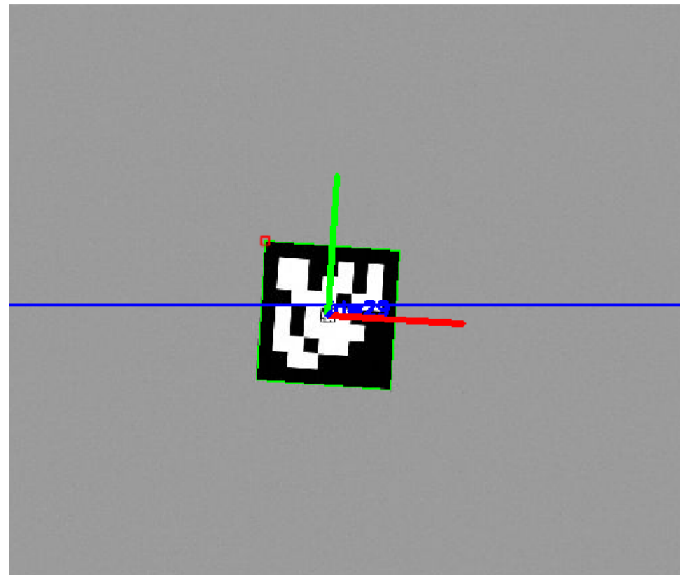
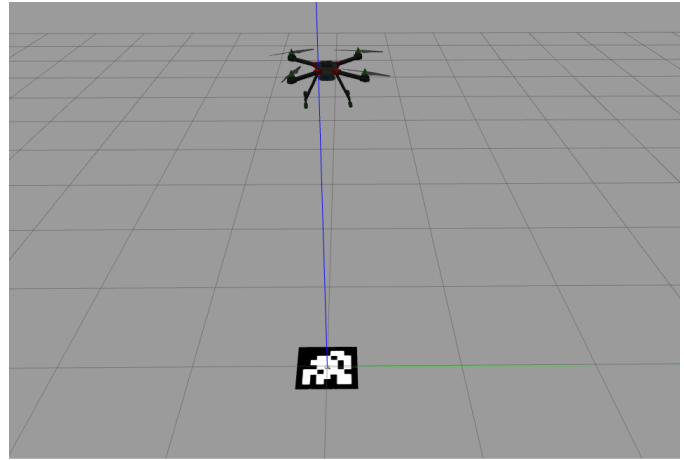


Fig. 5: The outer marker of the e-ArUco marker detected from the height of 2 meters. Detection is performed by the non-modified `aruco_detect` ROS package, which is commonly used for original ArUco markers detection.

B. Landing Procedure

The `aruco_detect` [33] ROS package is used to process camera frames and extract e-ArUco markers. This package finds ArUco markers in the image stream, publishes their vertices' (four corner points) coordinates, and computes the camera position relative to the marker. This package supports dictionaries with a different number of encoding bits (from 4x4 to 7x7). E-ArUco markers are based on ArUco markers of type 7x7. Such choice allows placing the inner marker directly in the center of the outer marker and does not affect the outer marker recognition.

Knowing a relative position of the camera with regard to the marker, a developed control software is capable to accurately navigate the UAV and land it on the e-ArUco marker. The landing algorithm works as follows. The UAV receives a

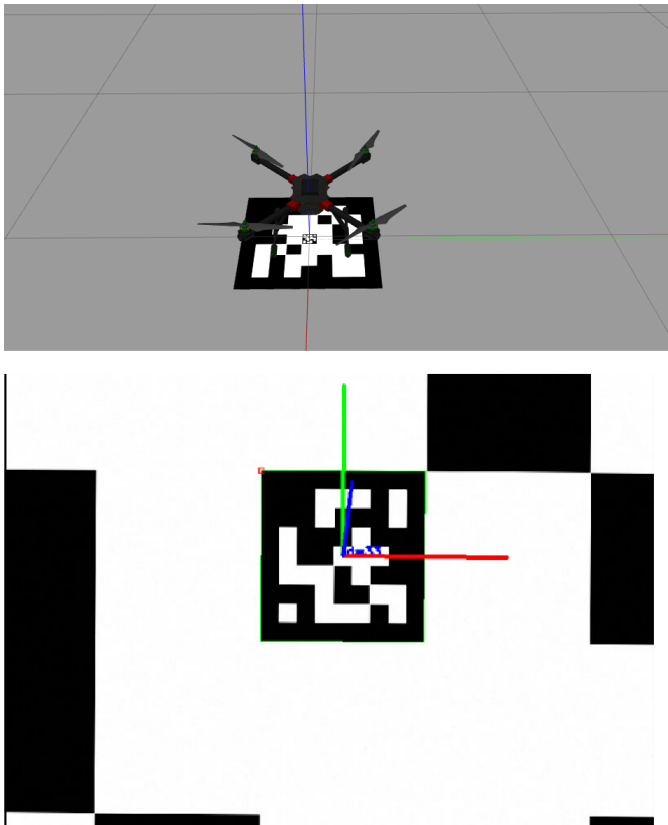


Fig. 6: The inner marker of the e-ArUco marker detected during last stages of landing. The outer marker is out of the frame and thus could not be detected.

command to land during a flight. The UAV starts searching for the e-ArUco marker. After a successful detection, the UAV aligns with a center of the outer ArUco and begins to descend. During the descending process, the UAV continuously adjusts its position in order to keep the detected marker in the center of the camera frame. As the marker becomes closer to the camera, the detection algorithm fails to detect the outer marker of e-ArUco. Instead, it switches to the inner marker detection and continues a precise positioning relying on the inner marker. The landing process is completed when the UAV touches the surface of the landing location.

V. EXPERIMENTAL VALIDATION

Multiple trials of landing experiments were carried out to evaluate effectiveness of the developed e-ArUco marker system. A total of 20 experiments were carried out in the Gazebo simulator. During the trial, the UAV took off to a height of 2 m and waited for the command to land on the e-ArUco marker (shown in Fig.5 and 6). After receiving the command, the UAV followed the above-mentioned landing procedure. When the landing was completed, the distance between the center of the UAV's camera and the e-ArUco marker's center was measured. Figure 7 demonstrates the

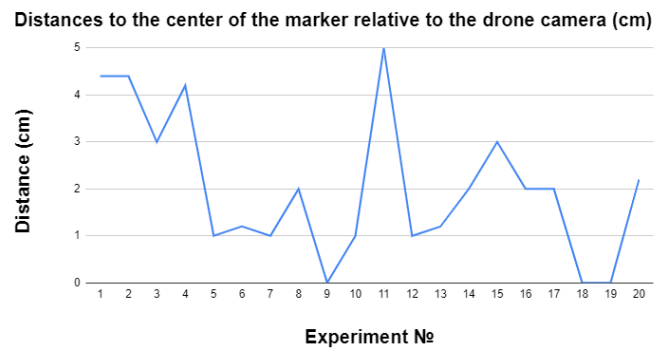


Fig. 7: Distances between the e-ArUco marker center and the center of the UAV camera (cm).

obtained distances within all trials. The average accuracy was 2.03 cm with a standard deviation of 1.53 cm.

VI. CONCLUSION

This paper presented a novel approach for precise UAV landing using visual sensory data. A new type of fiducial marker, embedded ArUco (e-ArUco) was developed specially for a task of a robust marker detection for a wide range of distances. E-ArUco markers are based on original ArUco markers approach and require only ArUco detection algorithms. The applicability of developed markers was validated using UAV landing experiments in a virtual environment. Both a developed marker and a landing algorithm were implemented within the ROS framework and tested in the Gazebo simulator. According to our virtual experiments, an average landing accuracy was 2.03 cm with a standard deviation of 1.53 cm.

ACKNOWLEDGMENT

This work was supported by the Russian Foundation for Basic Research (RFBR), project ID 19-58-70002. The forth author acknowledges the support of the Japan Science and Technology Agency, the JST Strategic International Collaborative Research Program, Project No. 18065977.

REFERENCES

- [1] D. Kingston, S. Rasmussen, and L. Humphrey, "Automated uav tasks for search and surveillance," in *2016 IEEE Conference on Control Applications (CCA)*. IEEE, 2016, pp. 1–8.
- [2] A. Danilov, U. D. Smirnov, and M. Pashkevich, "The system of the ecological monitoring of environment which is based on the usage of uav," *Russian journal of ecology*, vol. 46, no. 1, pp. 14–19, 2015.
- [3] S. Sankarasrinivasan, E. Balasubramanian, K. Karthik, U. Chandrasekar, and R. Gupta, "Health monitoring of civil structures with integrated uav and image processing system," *Procedia Computer Science*, vol. 54, pp. 508–515, 2015.
- [4] H. Shakhathreh, A. H. Sawalmeh, A. Al-Fuqaha, Z. Dou, E. Almaita, I. Khalil, N. S. Othman, A. Khreishah, and M. Guizani, "Unmanned aerial vehicles (uavs): A survey on civil applications and key research challenges," *Ieee Access*, vol. 7, pp. 48 572–48 634, 2019.
- [5] D. Levonevskiy, I. Vatamaniuk, and A. Saveliev, "Providing availability of the smart space services by means of incoming data control methods," in *International Conference on Interactive Collaborative Robotics*. Springer, 2018, pp. 170–180.

- [6] S. Emel'yanov, D. Makarov, A. I. Panov, and K. Yakovlev, "Multilayer cognitive architecture for uav control," *Cognitive Systems Research*, vol. 39, pp. 58–72, 2016.
- [7] A. Babinec, L. Jurišica, P. Hubinský, and F. Duchoň, "Visual localization of mobile robot using artificial markers," *Procedia Engineering*, vol. 96, pp. 1–9, 2014.
- [8] M. Irfan, S. Dalai, K. Kishore, S. Singh, and S. Akbar, "Vision-based guidance and navigation for autonomous mav in indoor environment," in *2020 11th International Conference on Computing, Communication and Networking Technologies (ICCCNT)*. IEEE, 2020, pp. 1–5.
- [9] E. Mingachev, R. Lavrenov, T. Tsoy, F. Matsuno, M. Svinin, J. Suthakorn, and E. Magid, "Comparison of ros-based monocular visual slam methods: Dso, Idso, orb-slam2 and dynaslam," in *International Conference on Interactive Collaborative Robotics*. Springer, 2020, pp. 222–233.
- [10] S. S. Tordal and G. Hovland, "Relative vessel motion tracking using sensor fusion, aruco markers, and mru sensors," *MODELING IDENTIFICATION AND CONTROL*, vol. 38, no. 2, pp. 79–93, 2017.
- [11] "Detection of ArUco Markers," https://docs.opencv.org/master/d5/dae/tutorial_aruco_detection.html.
- [12] A. Zakiev, K. Shabalina, T. Tsoy, and E. Magid, "Pilot virtual experiments on aruco and artag systems comparison for fiducial marker rotation resistance," in *Proceedings of 14th International Conference on Electromechanics and Robotics "Zavalishin's Readings"*. Springer, 2020, pp. 455–464.
- [13] S. Garrido-Jurado, R. Muñoz-Salinas, F. J. Madrid-Cuevas, and M. J. Marín-Jiménez, "Automatic generation and detection of highly reliable fiducial markers under occlusion," *Pattern Recognition*, vol. 47, no. 6, pp. 2280–2292, 2014.
- [14] P. Oščádal, D. Heczko, A. Vysocký, J. Mlotek, P. Novák, I. Virgala, M. Sukop, and Z. Bobovský, "Improved pose estimation of aruco tags using a novel 3d placement strategy," *Sensors*, vol. 20, no. 17, p. 4825, 2020.
- [15] R. Safin, E. Garipova, R. Lavrenov, H. Li, M. Svinin, and E. Magid, "Hardware and software video encoding comparison," in *2020 59th Annual Conference of the Society of Instrument and Control Engineers of Japan (SICE)*. IEEE, 2020, pp. 924–929.
- [16] M. F. Sani and G. Karimian, "Automatic navigation and landing of an indoor ar. drone quadrotor using aruco marker and inertial sensors," in *2017 International Conference on Computer and Drone Applications (IConDA)*. IEEE, 2017, pp. 102–107.
- [17] I. Lebedev, A. Erashov, and A. Shabanova, "Accurate autonomous uav landing using vision-based detection of aruco-marker," in *International Conference on Interactive Collaborative Robotics*. Springer, 2020, pp. 179–188.
- [18] A. Sagitov, K. Shabalina, L. Sabirova, H. Li, and E. Magid, "Artag, apriltag and caltag fiducial marker systems: Comparison in a presence of partial marker occlusion and rotation," in *ICINCO (2)*, 2017, pp. 182–191.
- [19] J. Wubben, F. Fabra, C. T. Calafate, T. Krzeszowski, J. M. Marquez-Barja, J.-C. Cano, and P. Manzoni, "Accurate landing of unmanned aerial vehicles using ground pattern recognition," *Electronics*, vol. 8, no. 12, p. 1532, 2019.
- [20] F. Fabra, C. T. Calafate, J. C. Cano, and P. Manzoni, "Ardusim: Accurate and real-time multicopter simulation," *Simulation Modelling Practice and Theory*, vol. 87, pp. 170–190, 2018.
- [21] C. Pan, T. Hu, and L. Shen, "Brisk based target localization for fixed-wing uav's vision-based autonomous landing," in *2015 IEEE International Conference on Information and Automation*. IEEE, 2015, pp. 2499–2503.
- [22] J. S. Wynn and T. W. McLain, "Visual servoing for multirotor precision landing in daylight and after-dark conditions," in *2019 International Conference on Unmanned Aircraft Systems (ICUAS)*. IEEE, 2019, pp. 1242–1248.
- [23] L. Meier, P. Tanskanen, L. Heng, G. H. Lee, F. Fraundorfer, and M. Pollefeys, "Pixhawk: A micro aerial vehicle design for autonomous flight using onboard computer vision," *Autonomous Robots*, vol. 33, no. 1-2, pp. 21–39, 2012.
- [24] L. Meier, D. Honegger, and M. Pollefeys, "Px4: A node-based multithreaded open source robotics framework for deeply embedded platforms," in *2015 IEEE international conference on robotics and automation (ICRA)*. IEEE, 2015, pp. 6235–6240.
- [25] R. Mittler, "Ros are good," *Trends in plant science*, vol. 22, no. 1, pp. 11–19, 2017.
- [26] "MAVROS," <https://github.com/mavlink/mavros>.
- [27] R. Petersen, *Ubuntu 19.04 Desktop: Applications and Administration*. surfing turtle press, 2019.
- [28] N. Koenig and A. Howard, "Design and use paradigms for gazebo, an open-source multi-robot simulator," in *2004 IEEE/RSJ International Conference on Intelligent Robots and Systems (IROS)(IEEE Cat. No. 04CH37566)*, vol. 3. IEEE, 2004, pp. 2149–2154.
- [29] B. Abbyasov, R. Lavrenov, A. Zakiev, K. Yakovlev, M. Svinin, and E. Magid, "Automatic tool for gazebo world construction: from a grayscale image to a 3d solid model," in *2020 IEEE International Conference on Robotics and Automation (ICRA)*. IEEE, 2020, pp. 7226–7232.
- [30] W. Z. Fum, "Implementation of simulink controller design on iris+ quadrotor," Naval Postgraduate School Monterey United States, Tech. Rep., 2015.
- [31] "hector quadrotor: Package Summary," http://wiki.ros.org/hector_quadrotor.
- [32] A. Sagitov, K. Shabalina, R. Lavrenov, and E. Magid, "Comparing fiducial marker systems in the presence of occlusion," in *2017 International Conference on Mechanical, System and Control Engineering (ICMSC)*. IEEE, 2017, pp. 377–382.
- [33] "aruco_detect ROS package," http://wiki.ros.org/aruco_detect.